Published in final edited form as:
Atherosclerosis. 2007 November ; 195(1): 75–82.

Anatomical Differences and Atherosclerosis in Apolipoprotein E - Deficient Mice with 129/SvEv and C57BL/6 Genetic Backgrounds

Nobuyo Maeda[1], **Lance Johnson**[1], **Shinja Kim**[1], **John Hagaman**[1], **Morton Friedman**[2], and **Robert Reddick**[3]

1*Department of Pathology and Laboratory Medicine, The University of North Carolina at Chapel Hill, Chapel Hill, NC 27599-7525, USA*

2*Department of Biomedical Engineering, Duke University, Durham, NC 27708-0281 USA*

3*Department of Pathology, University of Texas Health Sciences Center, San Antonio, TX 78284, USA*

Abstract

There are well-known genetic background effects on atherosclerosis susceptibility in mice. To study the basis of these effects, we have generated the apolipoprotein E-null mutation in mouse embryonic stem cells of 129/SvEv origin, maintained it in the inbred strain (129-apoE), and compared these mice with those previously made in strain 129/Ola and backcrossed to a C57BL/6 genetic background (B6-apoE). Plasma cholesterol and triglyceride levels in the apoE-129 mice are twice the levels in apoE-B6, and both VLDL/chylomicron remnants and HDL particles are increased. Regression analysis of plaque size relative to the age of mice suggests that the initiation of atherosclerotic plaque development at the aortic root is slower in 129-apoE mice (intercept at 3.9 mo in females and 4.1 mo in males) than in B6-apoE mice (1.3 mo in females and 2.8 mo in males). In contrast, 129-apoE mice develop extensive plaques in the aortic arches earlier than B6-apoE mice. Distinct differences in the geometry of the aortic arch between the two strains suggest that anatomical differences may contribute to the effects of genetic background on atherosclerosis. The 129-apoE/B6-apoE pair thus provides a tool to study factors governing the relation between arterial geometry and the location of plaque development.

Keywords

animal model; atherosclerotic plaque distribution; cholesterol; aortic arch; aortic root; inbred mouse strain; ductus arteriosus

Well-characterized animal models are essential for the study of common human diseases such as those involving the cardiovascular system. The first practical mouse model of atherosclerosis was developed by inactivating the gene coding for apolipoprotein E (apoE) (1-3). ApoE plays a central role in lipoprotein metabolism and is required for efficient receptor-mediated plasma clearance by the liver of chylomicron remnants and very low-density lipoprotein (VLDL)-remnant particles (4). Lack of apoE in the mutant mice results in an increased accumulation of cholesterol-enriched remnant particles and four times normal plasma cholesterol levels even

Correspondence to: Dr. Nobuyo Maeda, Department of Pathology and Laboratory Medicine, The University of North Carolina at Chapel Hill, 701 Brinkhous-Bullitt Building, Chapel Hill, NC 27599-7525. Phone: 919-966-6912, Fax: 919-966-8800. E-mail: nobuyo@med.unc.edu..

when the mice are fed regular low-fat, low-cholesterol chow. The apoE-deficient mice spontaneously develop atherosclerotic plaques similar to those seen in humans (5,6), with the exception that the spontaneous hemorrhage and rupture associated with the late stage human plaques have not been consistently observed in this model. ApoE-deficient mice, together with mice lacking LDL receptor (7), are widely used for atherosclerosis research.

The apoE-/- mice currently available from commercial sources (B6.129Apoe^{tm1UNC}) carry a deletion mutation that was originally made in our laboratory using embryonic stem (ES) cells derived from a strain 129/Ola mouse. The mutation was subsequently moved into a C57BL/6 (B6) genetic background by backcrossing to B6 for at least 10 generations. This extent of backcrossing ensures that the majority of the genome of the resulting mice is now of B6 origin. However, as in other mutant mice generated in 129 and backcrossed to B6, investigators need to take special care to eliminate the possibility that observed effects are due to strain differences in closely linked loci rather than to the mutation itself (8). Thus, while crosses between backcrossed apoE-/- mice and backcrossed mice carrying additional genetic alterations have been used extensively to discover genes and pathways that modify atherogenesis, a relatively large segment of genetic material surrounding the mutations is 129-derived in mutants but is B6-derived in wildtype controls. This type of consideration is particularly important when interpreting traits of apoE-/- mice that are quantitative and not directly explainable by the function of apoE in lipid metabolism. These include blood pressure (9), kidney damage (10), behavior (11), and susceptibility to infections (12,13). The observed phenotypes could be secondary to hyperlipidemia and/or atherosclerosis induced by lack of apoE, or the consequence of yet-to-be defined functions of apoE. However, it is also possible that the effects are the consequence of strain differences in genes tightly linked to the *Apoe* locus, since the apoE-/- mice carry a significant portion of chromosome 7 derived from 129/Ola, while the same portion of the wild type mice is derived from C57BL/6.

The simplest solution to these difficulties is to ensure that the mutations of interest are maintained in mice having the same genetic background as the ES cells in which the mutations are generated. Since the majority of new mutations have been made with strain 129 ES cells, the need to re-derive the apoE-null mutation in strain 129 ES cells becomes apparent. In this paper, we describe the development of atherosclerosis in the apoE-/- mice on a 129/SvEv genetic background (129-apoE) and compare them with apoE-/- mice backcrossed onto the B6 background (B6-apoE). We find that while 129-apoE mice begin to develop plaques at the aortic root later than B6-apoE mice, they develop more extensive lesions in the aortic arch.

Materials and methods

Mice

The gene targeting vector, pNMC109, the same DNA construct used in generating B6-apoE mice (1), was introduced into TC1 ES cells derived from 129/SvEvTac (gift from Dr. Leder at Harvard University). Chimeric males generated from the correctly targeted cells were mated with 129/SvEvTac females (Taconics Farm, Germantown, NY). Pups heterozygous for the disrupted *Apoe* locus were crossed once again with 129/SvEvTac wildtype mice and their heterozygous offspring were intercrossed to generate apoE-/- mice in a 129/SvEvTac background. Mice were maintained on a regular chow and experiments were carried out under protocols approved by the Institutional Animal Care and Use Committee of the University of North Carolina at Chapel Hill.

Plasma lipid analysis

Plasma was isolated, and total cholesterol and triglycerides were measured as described previously (14). Lipoproteins were separated from pooled plasma from at least six mice (1 ml)

into density fractions by ultracentrifugation, and subjected to SDS-PAGE analysis as described (15).

Atherosclerosis

Mice were sacrificed with an overdose of 2,2,2-tribromoethanol and perfusion fixed with 4% paraformaldehyde under a physiological pressure (pH.7.4). Frozen sections of proximal aorta and the part of the heart containing the aortic root, and plastic sections of arteries were made for morphological evaluation. Area of the atherosclerotic lesions was measured using NIH 1.59 Imaging Software and an average from four sections chosen by strict anatomical criteria was taken as the proximal aortic lesion size of each animal (6,14). To evaluate plaque formation in other parts of aorta, the aortic tree was dissected free of surrounding adventitial tissues and the plaques were visualized using a dissection microscope. Lesions at aortic arch were graded from one through ten.

Aortic Casting

Following anesthesia with a lethal dose of 2,2,2-tribromoethanol, the aorta of each mouse was catheterized with MRE 025 tubing (Braintree Scientific Inc., Braintree, MA) just proximal to the iliac bifurcation. The mouse was perfused with 3ml of saline containing 40unit/ml heparin followed by 1.5ml of freshly prepared casting material (Batson's No.17 Plastic Replica and Corrosion Kit, Polyscience Inc). A small puncture of the vena cava allowed draining and exit of excel casting material. Carcasses were placed for at 4°C overnight and subsequently placed in a maceration solution (saturated KOH) at 37°C with frequent volume changes to clear surrounding tissues.

Statistical Analysis

Data were collected from the 129-apoE mice having a median age of 6.7mo (2.5 – 22 mo old). The majority of the data for the B6-apoE (3.5 – 21 mo old, median age of 4.3mo) was compiled from those obtained from control animals in various experiments during the last 5 years in our laboratory. Statistical analyses were performed with the JMP software package (SAS Institute Inc., Cary, NC). Data are presented as mean ± SE.

Results

Generation of ApoE-deficient mice on 129SvEv background

The endogenous mouse *Apoe* gene was disrupted by homologous recombination between the targeting construct and the genomic DNA in ES cells derived from 129/SvEvTac. The recombination deleted parts of exon 3 and intron 3 from the endogenous mouse *Apoe* gene and replaced them with the neomycin resistance gene. The disruption of the native *Apoe* gene in 129-apoE mice is identical to that in the previously derived B6-apoE mice, and both resulting lines of mice lack apoE completely.

The body weight of the apoE-/- mice on a 129 inbred were slightly smaller than those of apoE +/+ littermates at 4 months of age, but the difference was not statistically significant (22.1±1.1 g for apoE+/+ females, n=10; 20.2±0.5 g for apoE-/- females, n=14; 24.2±0.8 g for apoE+/+ males, n=10; 23.0±0.7 g for apoE-/- males, n=13; P=0.05 for gender effect, P=0.5 for genotype effect by ANOVA). Body weights of 129-apoE male mice of age 4-6 months were significantly smaller than that in B6-apoE males (P<0.0001, Table 1) but body weights of females were not significantly different.

Plasma lipids and lipoproteins

We found differences in plasma lipid levels between 129-apoe and B6-apoE. Total plasma cholesterol levels are approximately 2.5 times higher in 129-apoE compared to B6-apoE mice (Table 1, $P<0.002$ for gender effect, $P<0.0001$ for strain effect, interaction not significant by two-way ANOVA). Similarly, plasma triglyceride levels in 129-apoE are twice as high as those in B6-apoE mice ($P<0.001$ for gender effect, $P<0.0001$ for strain effect, interaction not significant). Age had no effects on plasma lipid levels.

Fractionation of lipoproteins by ultracentrifugation showed that the cholesterol content in all the fractions was higher in 129-apoE mice than that in B6-apoE mice (Figure 1A). HDL-cholesterol ($1.10<d<1.21$) was approximately 2 times and VLDL-cholesterol ($d<1.006$) was about 1.5 times. There was a 2.6 fold increase of cholesterol in the fractions between $1.006<d<1.04$ indicating a marked increase of remnant particles in 129-apoE mice. Analysis of apolipoproteins in the density fractions by SDS-PAGE showed that the remnants accumulating in 129-apoE mice (sample 1 through 3 in Figure 1B) are mainly apoB48-containing particles. The amount of apoAIV associated with these remnants is also higher in 129-apoE mice than in B6-apoE mice. Since mice, unlike humans, make apoB48-containing particles in the liver as well as the intestine, the origin of the large-size lipoprotein particles in the 129-apoE mice is not certain. The increased amount of apoAI protein in the $1.10<d<1.21$ fraction (sample 7 in Fig 1B) is consistent with an increased levels of HDL in 129-apoE mice relative to B6-apoE mice.

Thus 129-apoE mice have twice as high plasma lipid levels as B6-apoE mice, as a consequence of increases in both apoB48 containing remnant particles and HDL.

Atherosclerosis at aortic root

Paigen *et al.* (16) showed that an atherogenic diet (15% fat, 1% cholesterol and 0.5% cholic acid) induces atherosclerotic lesions at the aortic roots in wildtype mice, and that 129 mice are mildly resistant while C57BL/6 mice are susceptible to this diet-induced atherosclerosis. In agreement with this, we find that the plaques at the aortic root area of 4-6 month old 129-apoE mice are significantly smaller than in B6-apoE mice as shown in table 1 despite the mean age of 5.4 mo in this group of 129-apoE was older than 4.3 mo in B6-apoE. The mean plaque size adjusted for age and gender by multiple regression analyses was 48,000±7,000 μm^2 in 129-apoE mice compared to 117,000±4,000 μm^2 in B6-apoE mice ($P<0.0001$). The difference was more prominent in females, where age adjusted mean lesion size in females was 52,000±9,000 μm^2 in 129-apoE-/- compared to 168,000±6,000 μm^2 in B6-apoE-/- ($P<0.0001$), while in males 38,000±8,000 μm^2 in 129-apoE compared to 64,000±4,000 μm^2 in B6-apoE mice ($P<0.01$). In addition, although there is a strong gender difference in plaque development between males and females in B6-apoE mice ($P<0.0001$), the gender difference was not significant in 129-apoE mice ($P=0.07$).

Figure 2 illustrates the mean lesion size at the aortic root of over 700 individual 129-apoE and B6-apoE animals relative to their age. Although the majority of the data was obtained from young mice, regression analysis shows an excellent linear relationship between the age of mice and lesion size with age accounting for 67 to 81% of the variance in lesion size of each group. Regression analysis also shows that the age-dependent enlargement of the plaques is not significantly different among the four groups (40 - 47,000 μm^2 per month). However, the intercepts on the X-axes differ: they are 3.9±0.4 in female and 4.1±0.4 in male 129-apoE mice compared to 1.3±0.3 in female and 2.8±0.3 in male B6-apoE mice. This implies that plaques at the aortic roots of B6-apoE mice start to develop earlier than in 129-apoE mice, and that B6-apoE females develop plaques earlier than B6-apoE males.

Microscopic views of plaques developing in the aortic root of the 129-apoE mice are complex and contain foam cells, fibrous caps, cholesterol clefts, calcifications and acellular necrotic cores (Supplementary Figure 1). The occurrence and extent of these features are similar in the two strains when similar size plaques are compared (not shown).

Together these data show that, although 129-apoE mice have higher plasma cholesterol and triglyceride levels, they begin to develop plaques within the aortic root later than B6-apoE mice. Our observation suggests that the strain and gender differences influencing the occurrence of aortic root lesions in of 129 and B6 mice are more likely related to the time of onset rather than to the subsequent increase in size of the plaques.

Atherosclerosis in aortic arch

In contrast to the later development of plaques in the aortic root of the 129-apoE mice, we found that in the aortic arch the 129-apoE mice develop extensive plaques earlier than B6-apoE mice. Figure 3 illustrates plaques visualized by Sudan IVB staining in the aortic arch of 6 mo old males with the two genetic backgrounds. (Plaques in the females were similar to those in males.) In the 129-apoE mice, lesions are clearly present at the branch points of the carotid arteries (left panels). In addition, extensive plaques are present on the surface of the inner curvature of the ascending aorta and the aortic arch. Plaques in the descending aorta are restricted to the proximal portion, and the remaining descending aortas of the 129-apoE mice at 6 months of age are relatively free from plaque development (not shown). In contrast, in the B6-apoE mice at 6 months of age (right panels), raised plaques are restricted to the brachiocephalic trunk (innominate artery) at the point where it branches from the aorta (blue arrow heads), although small plaques are also seen at the branching point of the left subclavian artery. Plaques on the surface of the inner curvature of the ascending aorta and the aortic arch are diffuse and thin. Grading the extent of lesions on a scale of 1 (restricted to one plaque at the brachiocephalic trunk) to 10 (the entire arch is covered with plaques, Supplementary Figure 2) showed that mean score of the 6 mo old 129-apoE mice (4.5±0.4, n=8) is significantly higher than that of the 6 mo old B6-apoE mice (1.8±0.3, n=8, $P<0.0001$). Grading also demonstrates the time-dependent development of the lesions in aortic arch in 129-apoE mice (Supplementary Figure 3). Microscopically, the lesions at branch points of the brachiocephalic trunk from 129-apoE mice contain similar components in the in B6-apoE mice with an exception that plaques of 129-apoE mice tend to contain more extensive cartilage than plaques of B6-apoE mice (Supplementary Figure 4). Plaques are observed in the descending aorta of older apoE-/- mice but their extent is not different between 129-apoE and B6-apoE mice.

The development of lesions on the aortic wall of the 129-apoE mice near the branching point of the left subclavian artery is particularly notable (Figure 3). Lesions in this area are already present in 3.5mo old 129-apoE mice but not seen in 8 mo old B6-apoE mice (not shown). This is immediately proximal to where the ductus arteriosus is attached to the descending aorta (indicated by arrows). Closure of the ductus arteriosus in many 129-apoE mice appears to be limited to its central portion, with the lumen still open on both the aortic and pulmonary artery portions of the ductus (Figure 4A). Plaque materials are present within these patent portions of the ductus (Figure 4B), and a cross section of the ductus arteriosus in a 129-apoE mouse shows plaque materials and calcification occluding the lumen but the medial layers being relatively intact (Figure 4C). In some animals, degenerative smooth muscle cells are evident and red blood cells are seen in the lumen (Figure 4D). In contrast, the ductus arteriosus in the B6-apoE mice appears completely fibrotic, being mainly composed of amorphous connective tissues and degenerated cells indicating that the closure was complete (Figure 4E).

There are other differences in the anatomy of vessels between the 129 and B6 mice, which are readily visualized by examining plastic casts of the aorta of wildtype mice of the two strains (Supplemental Figure 5). Casts made of four 129 and four B6 male mice at six months of age

showed that the diameters of the ascending, transversal, and descending portions of the aortic arch are approximately 20% smaller in the 129 than in the B6 mice (0.86±0.02 mm vs 1.02 ±0.1 mm, $P<0.05$). In addition, the mean length of brachiocephalic trunk (i.e. the distance between the branching from aorta to branching of right carotid and right subclavian arteries) is 40% shorter in 129 compared to B6 (0.9±0.1mm vs 1.3±0.1mm, $P<0.04$). Stereo-microscopic imaging of these and additional casts demonstrate that the aortic arch of the 129 strain shows a more symmetrical shape than that of the B6 strain (17). Detailed curvature measurements and calculations of the hemodynamics of arches of the B6 and129 strain of mice are in progress and will be reported elsewhere.

Thus, despite the slower start of plaque formation in the aortic root area, the 129-apoE mice develop plaques in the ascending aorta and aortic arch earlier than B6-apoE mice. This suggests that anatomical differences and geometry are important factors in strain differences of atherosclerosis susceptibility.

Discussion

We have characterized the development of atherosclerotic plaques in apoE-deficient mice on a pure inbred 129/SvEv genetic background and have compared it with the development of atherosclerosis in mice backcrossed for >10 generations onto a C57BL/6 genetic background. This comparison shows that factors governing the difference in atherosclerosis at aortic root between these two strains are related to the initiation of plaques rather than to their growth, and that the strain differences in atherosclerotic plaque development varies with the anatomical position examined.

The plasma levels of total cholesterol in the 129-apoE mice are higher than in B6-apoE mice, yet the plaque development at the aortic root of 129 apoE-mice is slower than in B6-apoE mice. While increased apoB-48 containing lipoproteins are atherogenic in the 129-apoE mice, increased HDL-cholesterol may overcome this adverse effect. The inverse relationship between elevated plasma lipids and reduced atherosclerosis has been reported previously in apoE-/- mice that have been backcrossed onto an FVB/NJ background (18). These authors analyzed an F2 population between apoE-/- mice on the FVB and B6 backgrounds, and found no correlation between the plasma levels of lipid/lipoproteins and the size of lesions at aortic root. This suggests that the strain differences that affect the susceptibility to atherosclerosis of the aortic root in these two strains of mice are independent from those determining plasma cholesterol levels. This conclusion is consistent with genetic mapping by Ishimori et al (19), who reported distinct loci affecting plasma HDL levels and atherosclerosis in high-fat diet fed wildtype C57BL/6J and wildtype 129/SvlmJ mice. These studies, however, did not investigate lesions in the aortic arch.

Our finding that 129-apoE mice with higher plasma lipids than B6-apoE mice develop atherosclerosis more slowly at the aortic root but faster within the aortic arch suggests that plaque formation is strongly influenced by anatomical location. The influence of hemodynamics on atheroma development has been discussed extensively, since areas prone to develop lesions coincide with areas of complex flow, such as areas on the inside of tight curves, near bifurcations and in areas where plaques are already present (20-23). Mice with different genetic backgrounds differ in many ways, including immune reaction and inflammatory responses (24), which may affect atherosclerosis differently at different vascular locations. However, no strain differences in the vascular anatomy of inbred mice has previously been considered in relation to atherosclerosis susceptibility, and relatively little attention has been paid to the postnatal development and geometry of the vasculature. Huang *et al*. have recently analyzed the geometry and mechanical properties of the aorta during postnatal development of C57BL/6 mice (25). They showed that the aorta was transformed from a cylindrical tube at

birth to a tapered structure during growth, adapting to the rapid change of blood pressure and blood flow after birth. Additionally, Topouzis and Majesky (26) have shown that the developmental origins of smooth muscle cells in different parts of large vessels in chick embryos are distinct and exhibit distinct gene expression patterns in response to various stimuli. These processes may differ from one strain to another in timing and in pattern, and in a gender dependent fashion, and may affect atherogenesis.

Strain difference in developmental programming is illustrated in the timing of the closure of ductus arteriosus, the arterial connection in the fetus between the pulmonary artery and the aorta. The ductus arteriosus closes following birth as a consequence of a complex process involving smooth muscle cell proliferation, migration and extracellular matrix deposition. Prostaglandins are important mediators for triggering this process, as demonstrated by the patent ductus and postnatal hypoxic death of mice lacking prostaglandin receptor E4 (26) and of mice lacking both cyclooxygenase 1 and 2 (27). Although we have not observed any postnatal death in our 129-apoE mice, we have found that both the aortic and pulmonary artery sides of the ductus arteriosus remain open in many of the adult 129-apoE mice and form funnel-like pockets. In some cases red blood cells are present in the lumen, and plaque materials (including calcifications, cholesterol crystals and foam cells) have been seen within these pockets. The influence of blood flow perturbation caused by such pockets is unlikely to extend to the wall very far, but together with the angles between the distal arch and descending aorta, it may be important for the formation of lesions in the aortic arch of 129-apoE mice.

In conclusion, while our comparison between B6 and 129 lines of apoE-/- mice does not explain the genetic factors underlying strain and gender differences, it underscores the need to investigate the relationship between anatomical differences and the development of atherosclerosis. Clearly, differences in blood vessel geometry and blood flow between 129-apoE and B6-apoE and other strains of mice need further investigation. In addition, our current description of strain differences in the geometries of the aortic arches of 129-apoE and B6-apoE- mice and their relationship to plaque formation provides a starting point for dissecting genetic factors that dictate vascular geometry and plaque formation. Finally, the apoE-deficient mice on a pure 129/SvEv background that we have developed here are useful for studying the atherogenic effects of new mutations made by gene targeting using 129 ES cells, since the issue of differences in genetic background influence is eliminated. Thus any phenotypes revealed in 129-apoE mice as such, or after crossing them with mice having additional mutations generated in strain 129 ES cells can be unequivocally ascribed to the consequence of the mutations themselves.

Supplementary Material

Refer to Web version on PubMed Central for supplementary material.

Acknowledgements

We thank Joshua Knowles, Jeffrey Hodgin, Yau-Sheng Tsai, Goeffrey Lewis, and Mathew Alexander for making their data available for analyses, Svetlana Zhilicheva and Jennifer Wilder, Kimberly Kluckman and Annette Staton for expert technical assistance. We thank Drs Oliver Smithies and Byron Ballou for useful comments. This work was supported by HL-42630 from the National Institutes of Health.

References

1. Piedrahita JA, Zhang SH, Hagaman JR, Oliver PM, Maeda N. Generation of mice carrying a mutant apolipoprotein E gene inactivated by gene targeting in embryonic stem cells. Proc Natl Acad Sci U S A 1992;89:4471–5. [PubMed: 1584779]

2. Plump AS, Smith JD, Hayek T, Aalto-Setala K, Walsh A, Verstuyft JG, Rubin EM, Breslow JL. Severe hypercholesterolemia and atherosclerosis in apolipoprotein E-deficient mice created by homologous recombination in ES cells. Cell 1992;71:343–53. [PubMed: 1423598]
3. Zhang SH, Reddick RL, Piedrahita JA, Maeda N. Spontaneous hypercholesterolemia and arterial lesions in mice lacking apolipoprotein E. Science 1992;258:468–71. [PubMed: 1411543]
4. Mahley RW. Apolipoprotein E: cholesterol transport protein with expanding role in cell biology. Science 1988;240:622–30. [PubMed: 3283935]
5. Nakashima Y, Plump AS, Raines EW, Breslow JL, Ross R. ApoE-deficient mice develop lesions of all phases of atherosclerosis throughout the arterial tree. Arterioscler Thromb 1994;14:133–40. [PubMed: 8274468]
6. Reddick RL, Zhang SH, Maeda N. Atherosclerosis in mice lacking apo E. Evaluation of lesional development and progression. Arterioscler Thromb 1994;14:141–7. [PubMed: 8274470]
7. Ishibashi S, Goldstein JL, Brown MS, Herz J, Burns DK. Massive xanthomatosis and atherosclerosis in cholesterol-fed low density lipoprotein receptor-negative mice. J Clin Invest 1994;93:1885–93. [PubMed: 8182121]
8. Knowles JW, Maeda N. Genetic modifiers of atherosclerosis in mice. Arterioscler Thromb Vasc Biol 2000;20:2336–45. [PubMed: 11073835]
9. Hartley CJ, Reddy AK, Madala S, Martin-McNulty B, Vergona R, Sullivan ME, Halks-Miller M, Taffet GE, Michael LH, Entman ML, Wang YX. Hemodynamic changes in apolipoprotein E-knockout mice. Am J Physiol Heart Circ Physiol 2000;279:H2326–34. [PubMed: 11045969]
10. Wen M, Segerer S, Dantas M, Brown PA, Hudkins KL, Goodpaster T, Kirk E, LeBoeuf RC, Alpers CE. Renal injury in apolipoprotein E-deficient mice. Lab Invest 2002;82:999–1006. [PubMed: 12177238]
11. McLachlan CS, Yi Xing Soh C. Differences in anxiety-related behavior between apolipoprotein E-deficient C57BL/6 and wild type C57BL/6 mice. Physiol Res 2005;54:701–4. [PubMed: 15717856]
12. Van Oosten M, Rensen PC, Van Amersfoort ES, Van Eck M, Van Dam AM, Breve JJ, Vogel T, Panet A, Van Berkel TJ, Kuiper J. Apolipoprotein E protects against bacterial lipopolysaccharide-induced lethality. A new therapeutic approach to treat gram-negative sepsis. J Biol Chem 2001;276:8820–4. [PubMed: 11136731]
13. Vonk AG, De Bont N, Netea MG, Demacker PN, van der Meer JW, Stalenhoef AF, Kullberg BJ. Apolipoprotein-E-deficient mice exhibit an increased susceptibility to disseminated candidiasis. Med Mycol 2004;42:341–8. [PubMed: 15473359]
14. Zhang SH, Reddick RL, Burkey B, Maeda N. Diet-induced atherosclerosis in mice heterozygous and homozygous for apolipoprotein E gene disruption. J Clin Invest 1994;94:937–45. [PubMed: 8083379]
15. Knouff C, Hinsdale ME, Mezdour H, Altenburg MK, Watanabe M, Quarfordt SH, Sullivan PM, Maeda N. Apo E structure determines VLDL clearance and atherosclerosis risk in mice. J Clin Invest 1999;103:1579–86. [PubMed: 10359567]
16. Paigen B, Morrow A, Brandon C, Mitchell D, Holmes P. Variation in susceptibility to atherosclerosis among inbred strains of mice. Atherosclerosis 1985;57:65–73. [PubMed: 3841001]
17. Zhu, H.; Shih, J.; Long, DS.; Maeda, N.; Hageman, JR.; Friedman, MH. Characterizing 3-D geometry of mouse aortic arch using light stereo-microscopic imaging. Proc.28th IEEE EMBS Ann. Int'l Conf.; New York. August-September 2006;
18. Dansky HM, Charlton SA, Sikes JL, Heath SC, Simantov R, Levin LF, Shu P, Moore KJ, Breslow JL, Smith JD. Genetic background determines the extent of atherosclerosis in ApoE-deficient mice. Arterioscler Thromb Vasc Biol 1999;19:1960–8. [PubMed: 10446078]
19. Ishimori N, Li R, Kelmenson PM, Korstanje R, Walsh KA, Churchill GA, Forsman-Semb K, Paigen B. Quantitative trait loci analysis for plasma HDL-cholesterol concentrations and atherosclerosis susceptibility between inbred mouse strains C57BL/6J and 129S1/SvImJ. Arterioscler Thromb Vasc Biol 2004;24:161–6. [PubMed: 14592847]
20. Caro CG, Fitz-Gerald JM, Schroter RC. Arterial wall shear and distribution of early atheroma in man. Nature 1969;223:1159–61. [PubMed: 5810692]

21. Friedman MH, Hutchins GM, Bargeron CB, Deters OJ, Mark FF. Correlation of human arterial morphology with hemodynamic measurements in arterial casts. J Biomech Eng 1981;103:204–7. [PubMed: 7278199]

22. Ku DN, Giddens DP, Zarins CK, Glagov S. Pulsatile flow and atherosclerosis in the human carotid bifurcation. Arteriosclerosis 1985;5:293–302. [PubMed: 3994585]

23. DeBakey ME, Lawrie GM, Gleaser DH. Patterns of atherosclerosis and their surgical significance. Ann Surg 1985;201:115–31. [PubMed: 3155934]

24. Tabibiazar R, Wagner RA, Spin JM, Ashley EA, Narasimhan B, Rubin EM, Efron B, Tsao PS, Tibshirani R, Quertermous T. Mouse strain-specific differences in vascular wall gene expression and their relationship to vascular disease. Arterioscler Thromb Vasc Biol 2005;25:302–8. [PubMed: 15550693]

25. Huang Y, Guo X, Kassab GS. Axial nonuniformity of geometric and mechanical properties of mouse aorta is increased during postnatal growth. Am J Physiol Heart Circ Physiol 2006;290:H657–64. [PubMed: 16172154]

26. Topouzis S, Majesky MW. Smooth Muscle Lineage Diversity in the Chick Embryo. Dev Biol 1996;178:430–45.

27. Nguyen M, Camenisch T, Snouwaert JN, Hicks E, Coffman TM, Anderson PA, Malouf NN, Koller BH. The prostaglandin receptor EP4 triggers remodelling of the cardiovascular system at birth. Nature 1997;390:78–81. [PubMed: 9363893]

28. Loftin CD, Trivedi DB, Tiano HF, Clark JA, Lee CA, Epstein JA, Morham SG, Breyer MD, Nguyen M, Hawkins BM, Goulet JL, Smithies O, Koller BH, Langenbach R. Failure of ductus arteriosus closure and remodeling in neonatal mice deficient in cyclooxygenase-1 and cyclooxygenase-2. Proc Natl Acad Sci U S A 2001;98:1059–64. [PubMed: 11158594]

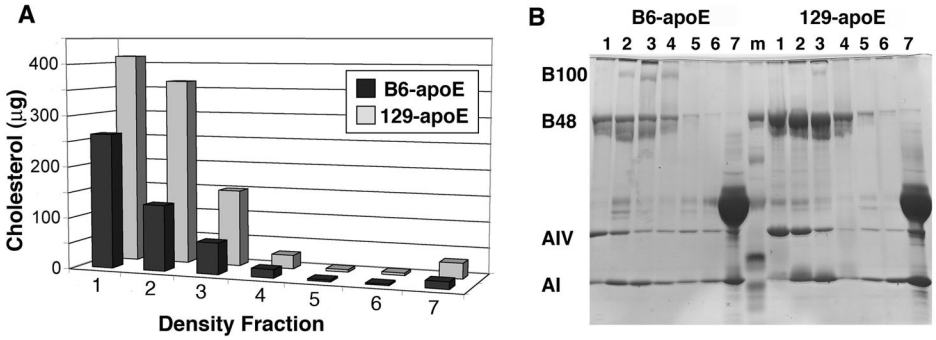

Figure 1.

Plasma lipoprotein and apolipoprotein distributions. Plasma pooled from six mice (1ml) was separated by serial ultracentrifugation into density fractions: 1, d<1.006; 2, 1.006<d<1.02; 3, 1.02<d<1.04; 4. 1.04<d<1.06; 5, 1.06<d<1.08; 6, 1.08<d<1.10; and 7, 1.10<d<1.21. (A) Cholesterol content of each density fraction from B6-apoE mice (black bars) and 129-apoE mice (grey bars). (B) Equal volumes of the fractions 1 through 7 were subjected to SDS-PAGE electrophoresis and stained by Coomassie Brilliant Blue. The positions of apolipoprotein B100, B48, AIV and AI are indicated.

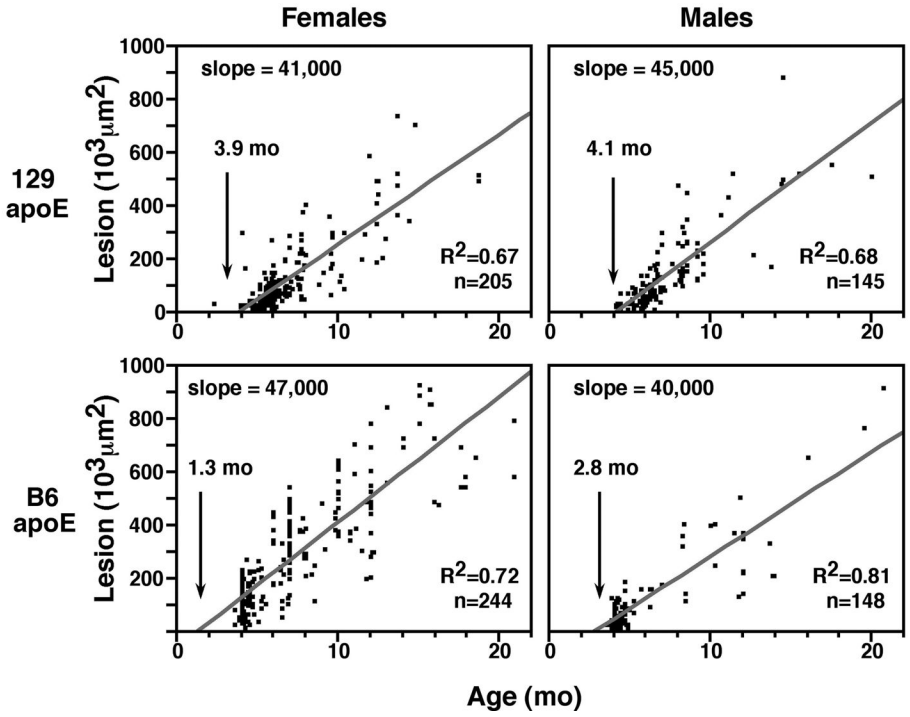

Figure 2.

Relationships between age and size of plaques at the aortic roots of apoE-/- mice having 129/SvEv and C57BL/6 genetic backgrounds. The slopes of the lines (40,000 - 47,000) fitted by linear least-squares regression represent the growth of plaques (in μm^2 per month), and the X-axis intercepts (1.3 – 4.1 mo) represent the time when plaques were initiated. n, number of animals.

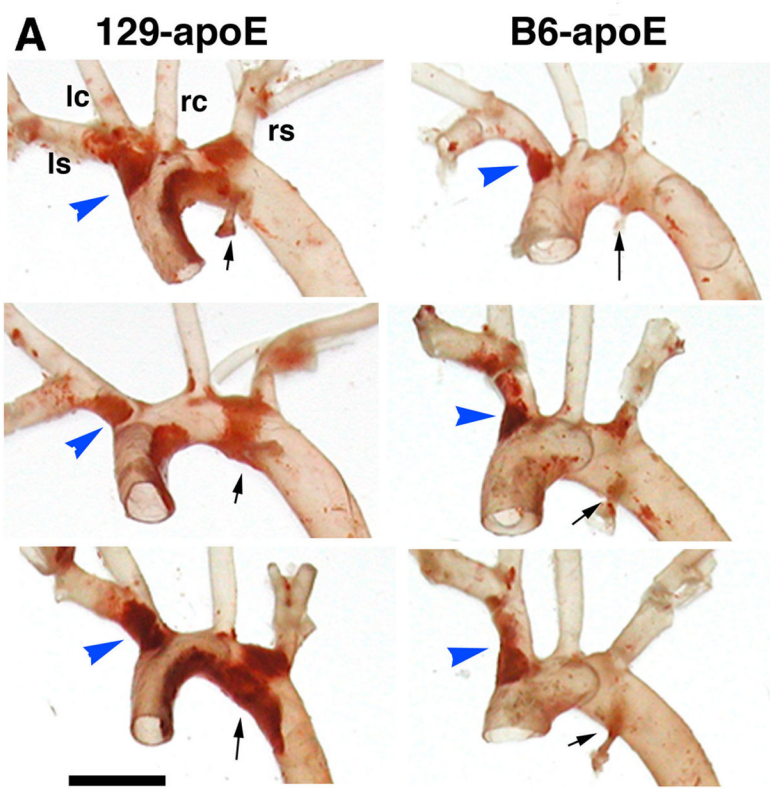

Figure 3.

Aortic arch and atherosclerosis. Atherosclerotic lesions in the aortic arches of three 129-apoE (left panels) and three B6-apoE (right panels) mice stained red with Sudan IVB. Note that the brachiocephalic trunks (blue arrowheads) are longer in B6-apoE than in 129-apoE mice. The attachment site of the ductus arteriosus to each aorta is indicated by a small black arrow. The black bar is 0.2 mm. lc, left common carotid artery; ls, left subclavian artery, rc, right common carotid artery; rs, right subclavian artery.

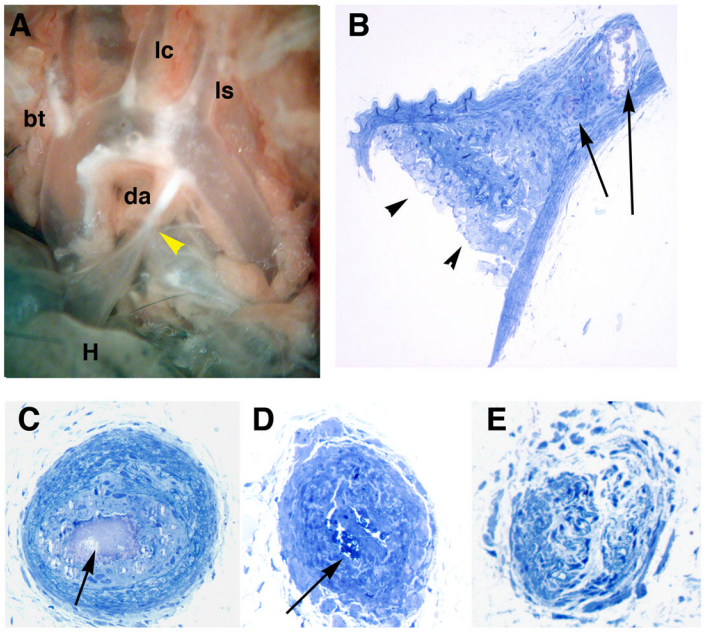

Figure 4.

Plaques within the ductus arteriosus of 129-apoE mice. (A), aortic arch and ductus arteriosus in a 6 mo old 129-apoE female. Plaques are visible through the aortic wall as shiny white areas. H, heart; bt, brachiocephalic trunk; lc, left common carotid artery; ls, left subclavian artery. The ductus arteriosus (da) has a funnel-like opening at its pulmonary end (yellow arrowhead). The whiteness towards the aortic side of the ductus arteriosus indicates plaques filling the ductus. (B), longitudinal section showing the opening to the pulmonary artery side of the ductus arteriosus of a 6 mo old male 129-apoE mouse. Plaque materials within the lumen are covered with foam cells (arrowheads). Calcified materials are filling the lumen of the aortic side (arrows). Plastic section, stained with Toluidine blue. 20X. (C), cross section of the ductus arteriosus of the same animal as (B) at the aortic attachment end. The lumen contains smooth muscle cells and calcified materials (arrow). 40X. (D), cross section of the ductus arteiosus from another 6 mo old 129-apoE male showing degenerative changes of smooth muscle cells. The arrow indicates red blood cells in the lumen. 40X. (E), a cross section of the ductus arteriosus of a 5 mo old B6-apoE male showing complete obliteration of the vascular structure and fibrotic alterations.

Table 1

Plasma Lipids and Lesions at the Aortic Root of ApoE-/- Mice of 4-6 mo of Age.

	129-apoE-/-		B6-apoE-/-		Effects (*P*)	
	Female	Male	Female	Male	Strain	Gender
Age (month)	5.4±0.1 (115)	5.4±0.1 (66)	4.4±0.1 (149)	4.3±0.1 (148)	--	--
BW (g)	22.8±0.2 (109)	26.4±0.3 (63)	22.4±0.2 (101)	28.9±0.4 (79)	<0.0001	<0.0001
CH (mg/dl)	709±21 (101)	744±28 (60)	295±8 (79)	350±11 (90)	<0.0001	<0.002
TG (mg/dl)	120±7 (60)	185±20 (53)	60±3 (61)	84±4 (76)	<0.001	<0.001
Lesion size ($10^3\mu m^2$)	64±5 (104)	51±4 (63)	131±7 (136)	55±3 (126)	<0.0001	<0.0001

Values are mean ± S.E. BW, body weight; CH, total cholesterol; TG, triglycerides. Only the mice with between 4 and 8 mo of age were included in this table. The numbers in parentheses indicate the number of mice.

Statistical analysis was by ANOVA. Body weight differs significantly in males but not in females. Lesion size was analyzed including age as a co-factor. Effects of gender on lesion size was significant in B6-apoE but not in 129-apoE.